Advances in Science and Technology, Vol. 8, No. 1, March / April, 2014, pp 23 - 34

Cosmological Evolution in Extended Extragalactic Radio Sources

C. C. Onuchukwu*
Department of Industrial Physics, Anambra State University, Uli, Anambra State, Nigeria.
(Submitted: December 20, 2013; Accepted: April 23, 2014)

Abstract

We carried out comparative statistical analyses some of the observed and calculated parameters of high luminosity FR-II radio galaxies and radio-loud quasars which include the extended linear size (D), the extended luminosity (P), spectral index (α), redshift (z), bending angle (ϕ), apparent flux ratio (R), core-dominance parameter (R^*) and arm-length ratio (Q) in order to investigate the phenomenon of cosmological evolution in extragalactic radio sources. The $P - z$ relation shows a strong correlation (with correlation coefficient $r = 0.9$), which can be attributed to a strong selection effect. The linear regression analyses carried out on the selected samples indicate that the extended linear size and extended luminosity undergo similar evolution with redshift (z) for both radio-loud quasars and FR-II radio galaxies. On assuming that the de-projected linear sizes of FR-II radio galaxy and radio-loud quasars are similar when matched in z, we obtained a foreshortening factor $F = 1.87$ for $0.003 \leq z \leq 2.880$, which is consistent with the radio-loud quasars and FR-II radio galaxy unification scheme.

Keywords: Galaxies – General, Active; Method – Statistical, Data Analysis

1.0 Introduction

Observations of extragalactic radio sources (EGRSs) show that their appearances depend strongly on orientations, thus, most classification schemes are based on aspect dependent properties than intrinsic properties like the black hole mass and spin. Thus, unifying these apparently different yet intrinsically similar objects is important in the understanding of the physics of extragalactic radio sources. Different unification schemes have been applied to EGRS (e.g. Barthel 1989; Antonucci 1993; Urry & Padovani 1995). These unification schemes are based on the concept of opaque and obscuring torus that surrounds a central engine and the relativistic Doppler boosting of radiation beamed to the line of sight of a distant observer. The generally acceptable structure of EGRS, assumed that the central engine (possibly a super massive black hole) powers the EGRS luminosity (Blandford & Znajek 1977; Blandford & Payne1982; Magorrian *et al*., 1998; Liu *et al*. 2006; Lobanov & Zensus 2006) by its gravitational potential energy. Matter accretes towards the galactic center, loses angular momentum through turbulent processes in an accretion disk with outflow of energetic particles occurring along the poles of the disk or torus, escaping and forming collimated radio-emitting jets (Blandford & Payne 1982; Urry & Padovani 1995; Lobanov & Zensus 2006). The plasma in the jets, at least on the smallest scales, streams out at very high velocities (Kellermann *et al*. 2004; Piner *et al*. 2007; Britzen *et al*. 2008).

One very interesting model of EGRS unification is based on geometric idea by Barthel (1989), which seeks to unify radio-loud quasars and FR-II radio galaxies in the Fanarof & Riley (1974) radio luminosity classification. This model is motivated by the suggestion from observational data, that the angular extent of emission and number densities from quasars are less than that from FR-II radio galaxies. Several authors (Antonucci 1993; Urry and Padovani, 1995; Willot *et al*. 1998; Nilsson, 1998; Ubachukwu & Ogwo, 1998; Ubachukwu, 2002) have analyzed this model using various observable parameters. One major contrary view to the unification of radio-loud quasars and FR-II galaxies comes from the environmental aspect. Smith & Heckman (1989) showed that statistically, the host galaxies of radio-loud quasars and FR-II galaxies are different, in contrast with the result of Lehnert *et*

***Author's e-mail address:** onuchukwu71chika@yahoo.com

al. (1992), which indicates that the host galaxy population statistics may be similar. McCarthy *et al*. (1995), found a correlation between the radio emission and the optical emission luminosities, but in many instances, this optical emission is believed to be intrinsically asymmetric. Yet McCarthy *et al*. (1995) found a strong correlation between the radio and optical emission data, in the sense that the brightest optical emission lies on the side of the radio lobe that is normally deduced to be "closer" from the beaming arguments. This would imply that, at least, some of the radio asymmetry is also intrinsic, which is contrary to the assumption of unification.

In this study, we will investigate the unification scheme of high luminosity radio galaxies (FR-II) and radio-loud quasars by analyzing the relationships between some of the observed and calculated parameters – linear size (D), Luminosity (P), redshift (z) and spectral index (α) and the variation with asymmetry parameters (arm-length ratio (Q), apparent flux ratio (R), bending angle (ϕ) and core-dominance parameter (R^*)). We believe that our study will reveal any basic/intrinsic difference between radio galaxies (FR-II) and radio-loud quasars.

2.0 Data, Analyses and Results

2.1 Data

Our analyses were based on a sample of radio loud-quasars and high luminosity FR II radio galaxies obtained from Nilsson (1998). The original sample consisted of 1038 sources, 544 FR–II radio galaxies, 329 as radio-loud quasars and 165 sources with no optical classification. We selected all the FR-II radio galaxies and radio-loud quasars with complete structural and cosmological information – linear size (D), luminosity (P), spectral index (α), redshift (z) and asymmetry parameters. The redshift range is $0.003 \leq z \leq 4.250$, the linear sizes are in the range $0.3 \leq D(kpc) \leq 5853.3\ kpc$, spectral index lie in the range $0.10 \leq \alpha \leq 1.62$ and extended radio luminosity (measured in $erg\ s^{-1}$) lie in the range $38.38 \leq \log P_{(178\ MHz)} \leq 46\ 24$. The sample is heterogeneous and suitable for population study of radio sources with various characteristics. The final sample consisted of 334 FR-II galaxies and 336 radio-loud quasars.

2.2 Analyses and Results

2.2.1 Distribution of Parameters of High Luminosity FR-II Radio Galaxies and Radio-Loud Quasars

Figures 1 to 8 show the distribution plots of the extended linear size (D), extended luminosity (P), spectral index (α), redshift (z), arm-length ratio (Q), bending angle (ϕ), apparent flux ratio (R) and core-dominance parameter (R^*) of both the radio-loud quasars (solid line) and FR-II galaxies (dotted line). The linear size distribution plot shows that generally, galaxies (with $\log D_{\mathrm{m}} = 2.4 \pm 0.4\ kpc$) have larger projected linear size than quasars (with $\log D_{\mathrm{m}} = 2.1 \pm 0.4\ kpc$), but are generally nearer with $\log(1 + z_{\mathrm{m}}) = 0.13 \pm 0.10$ while for quasars, $\log(1 + z_{\mathrm{m}}) = 0.29 \pm 0.11$ (here and elsewhere the subscript m indicates the average value). The luminosity distribution indicates that quasars are in general more luminous than galaxies; with $\log P_{\mathrm{m}} = 44.5 \pm 0.6$ for quasars and $\log P_{\mathrm{m}} = 43.4 \pm 0.8$ for galaxies. The distribution plots of the asymmetry parameters (Q, ϕ, R and R^*) indicate that radio loud quasars are more asymmetric than FR-II radio galaxies with $R^*_{\mathrm{m}} = 0.3 \pm 0.2$, $Q_{\mathrm{m}} = 1.6 \pm 0.5$, $\phi_{\mathrm{m}} = 15 \pm 10$ and $R_{\mathrm{m}} = 2.0 \pm 1.0$ for quasars with $R^*_{\mathrm{m}} = 0.2 \pm 0.1$, $Q_{\mathrm{m}} = 1.4 \pm 0.3$, $\phi_{\mathrm{m}} = 9 \pm 8$ and $R_{\mathrm{m}} = 1.1 \pm 0.6$ for galaxies, The quoted errors are the standard error associated with the observed/calculated values of the parameter. Barthel (1989) concluded that the higher values of asymmetry parameters observed for quasars than FR-II radio galaxies is due to orientation rather than being intrinsic. The spectral index for both classes of sources shows similar distribution. Barthel (1989) concluded that the higher values of asymmetry parameters observed for quasars than FR-II radio galaxies is due to orientation rather than being intrinsic. The spectral index for both classes of sources shows similar distribution.

In Figures 9 – 15, we display the log – log scatter plots of the observed/calculated parameters we ana-

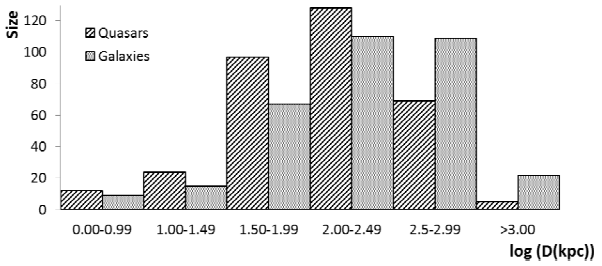

Figure 1: Distribution Plot of Extended Linear Size for the Sample of 334 FR-II Radio Galaxies and 336 Radio-Loud Quasars. (Key: Slanted Line Filled Bar = Quasars: Dotted Filled Bar = Galaxies).

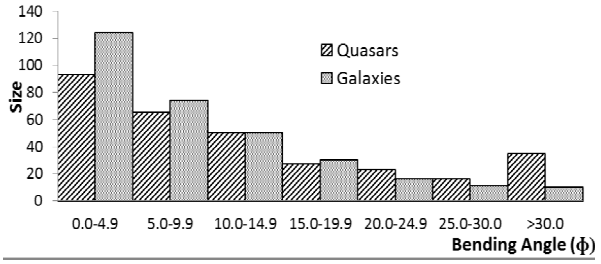

Figure 5: Distribution Plot of Bending Angle for the Sample of 313 FR-II Radio Galaxies and 308 Radio-Loud Quasars. (Key: Slanted Line Filled Bar = Quasars: Dotted Filled Bar = Galaxies).

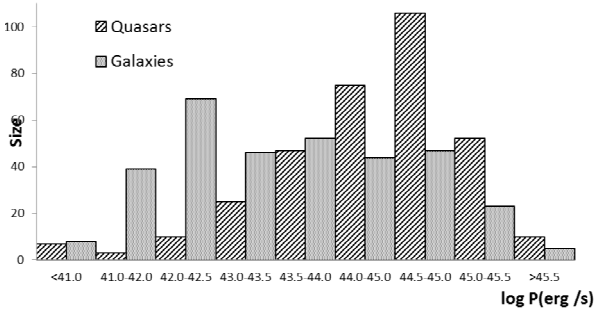

Figure 2: Distribution Plot of Extended Luminosity Size for the Sample of 334 FR-II Radio Galaxies and 336 Radio-Loud Quasars. (Key: Slanted Line Filled Bar = Quasars: Dotted Filled Bar = Galaxies).

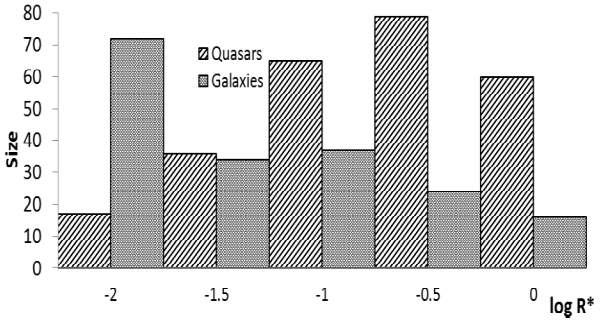

Figure 6: Distribution Plot of Core-Dominance Parameter for the Sample of 183 FR-II Radio Galaxies and 257 Radio-Loud Quasars. (Key: Slanted Line Filled Bar = Quasars: Dotted Filled Bar = Galaxies).

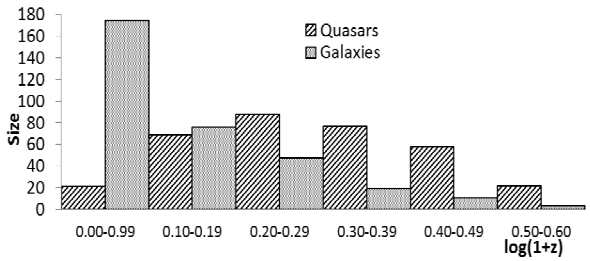

Figure 3: Distribution Plot of Redshift for the Sample of 334 FR-II Radio Galaxies and 336 Radio-Loud Quasars. (Key: Slanted Line Filled Bar = Quasars: Dotted Filled Bar = Galaxies).

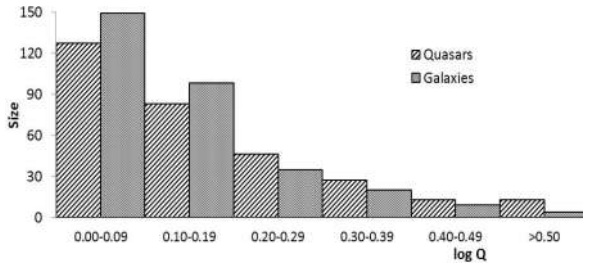

Figure 7: Distribution Plot of Arm-Length Ratio for the Sample of 313 FR-II Radio Galaxies and 308 Radio-Loud Quasars. (Key: Slanted Line Filled Bar = Quasars: Dotted Filled Bar = Galaxies).

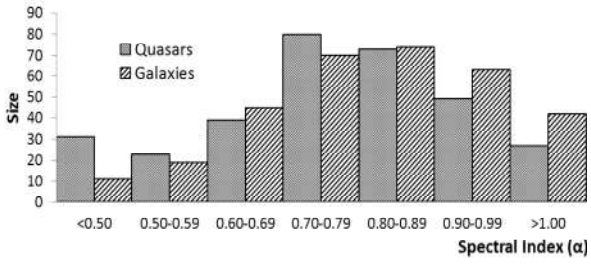

Figure 4: Distribution Plot of Spectral Index for the Sample of 334 FR-II Radio Galaxies and 336 Radio-Loud Quasars. (Key: Slanted Line Filled Bar = Quasars: Dotted Filled Bar = Galaxies).

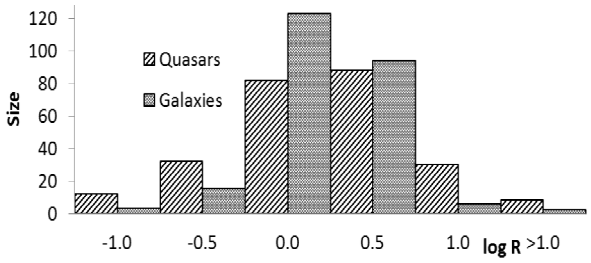

Figure 8: Distribution Plot of Apparent Flux Ratio for the Sample of 242 FR-II Radio Galaxies and 253 Radio-Loud Quasars. (Key: Slanted Line Filled Bar = Quasars: Dotted Filled Bar = Galaxies).

lyzed for FR-II radio galaxies and radio-loud quasars. Figure 9 is the plot of $\log\alpha$ against $\log(1+z)$. The plot shows no observable trend in the variation of α with z for quasars, a regression fit gives $\alpha \propto (1+z)^{0.2\pm0.1}$ with $r = 0.1$; for galaxies, the plot seems to shows some form of apparent increase in α with z, regression analysis gives $\alpha \propto (1+z)^{0.4\pm0.1}$ with $r = 0.4$, where r is the correlation coefficient. Figure 10 is the plot of projected linear size (D) against redshift (z) and shows that linear size decreases with redshift for both quasars and galaxies. A regression fit to the $D - z$ data gives: $D \propto (1+z)^{-0.76\pm0.13}$ with $r = -0.3$ and $D \propto (1+z)^{-0.99\pm0.12}$ with $r = -0.2$ respectively for quasars and galaxies. Figure 11 is the plot of P against z, and like all flux density limited sample, it showed a strong correlation between P and z usually attributed to Malquist bias. Regression fit to the $P - z$ data gives: $P \propto (1+z)^{2.1\pm0.5}$ with $r = 0.7$ and $P \propto (1+z)^{3.5\pm0.3}$ with $r = 0.8$ respectively for quasars and galaxies. The regression fit suggests a stronger $P - z$ evolution for galaxies than for quasars. Figure 12 is the plot of R^* against z. Galaxies Galaxies show stronger decrease of R^* with z than quasars. Regression fit to the $R^* - z$ data gives $R^* \propto (1+z)^{-3.5\pm0.5}$ with $r = -0.5$ and $R^* \propto (1+z)^{-0.6\pm0.2}$ with $r = -0.2$ for galaxies and quasars respectively. Figure 13 shows the plot of $Q - z$ data, indicating no appreciable cosmological evolution of arm-length ratio with redshift for FR-II galaxies and quasars, with regression fit giving $Q \propto (1+z)^{0.2\pm0.1}$ with $r = -0.2$ for quasar and $Q \propto (1+z)^{0.1\pm0.1}$ with $r = -0.2$ for galaxies. Figure 14 is the plot of R against z and it indicates no cosmological evolution in R. A linear regression analysis of the data seems to suggest a tendency for the apparent flux ratio with redshift for quasars while it decreases for galaxies. The regression fit gives $R \propto (1+z)^{0.6\pm0.2}$ with $r = -0.1$ for quasars and $R \propto (1+z)^{-0.2\pm0.1}$ with $r = -0.1$ for galaxies. Figure 15 is the plot of $\phi - z$ data on logarithmic scale. There is no apparent dependence of bending angle on redshift for both classes of objects.

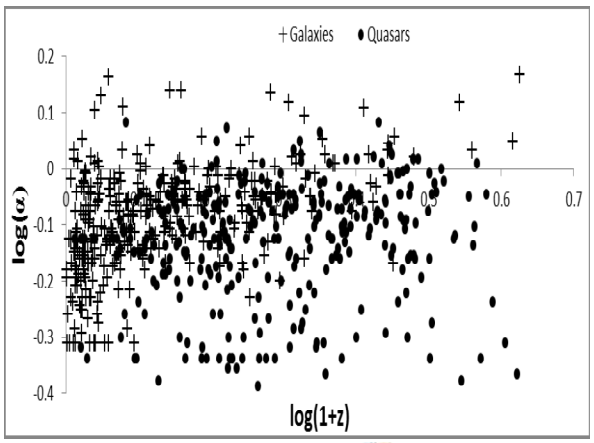

Scatter Plot of spectral Index (α) against Redshift (z) on Logarithm Scale for the Sample of 334 FR-II Radio Galaxies and 336 Radio-Loud Quasars. (Key: • = Quasars: + = Galaxies)

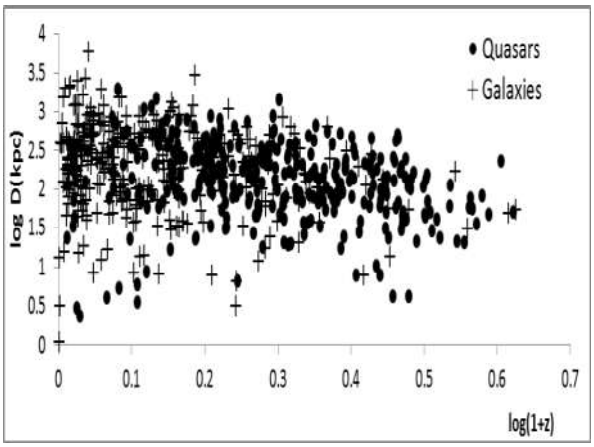

Figure 10: A Scatter Plot of Linear Size $(D(kpc))$ Against Redshift (z) on Logarithm Scale for the Sample of 334 FR-II Radio Galaxies and 336 Radio-Loud Quasars. (Key: •= Quasars: + = Galaxies).

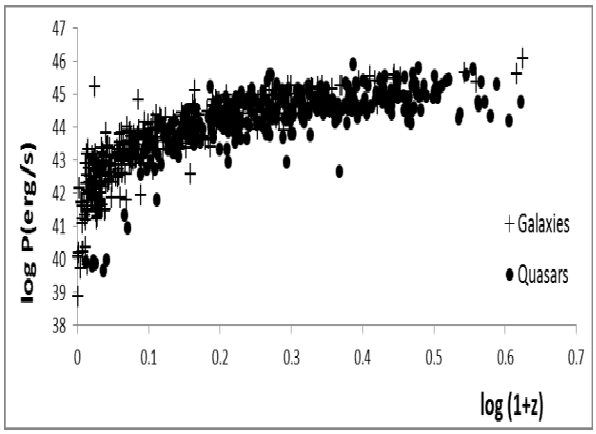

Figure 11: A Scatter Plot of Extended Lumionosity (P) Against Redshift (z) on Logarithm Scale for the Sample of 334 FR-II Radio Galaxies and 336 Radio-Loud Quasars. (Key: •= Quasars: + = Galaxies).

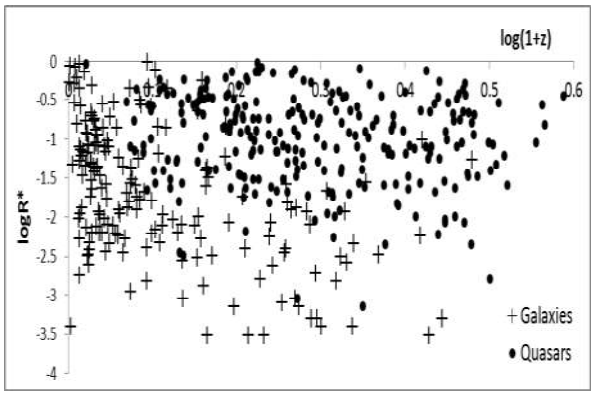

Figure 12: A Scatter Plot of Core-Dominace Parameter (R^*) Against Redshift (z) on Logarithm Scale for the Sample of 183 FR-II Radio Galaxies and 257 Radio-Loud Quasars. (Key: •= Quasars: + = Galaxies).

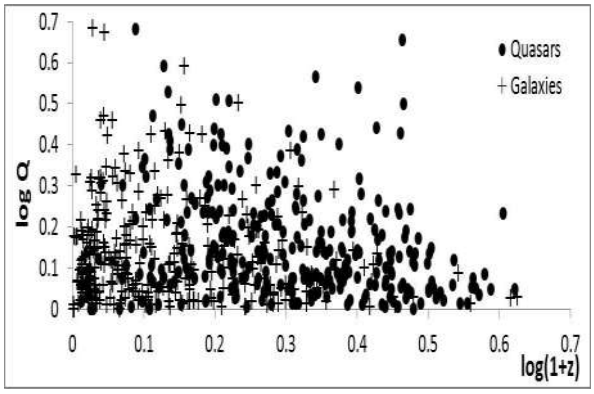

Figure 13: A Scatter Plot of Arm-Length Ratio (Q) Against Redshift (z) on Logarithm Scale for the Sample of 313 FR-II Radio Galaxies and 308 Radio-Loud Quasars. (Key: •= Quasars: + = Galaxies).

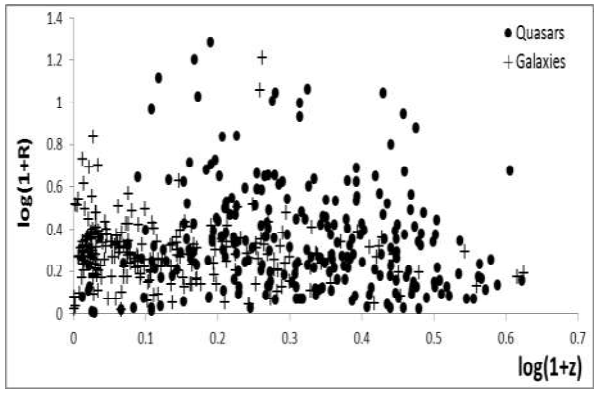

Figure 14: A Scatter Plot of Apparent Luminosity Flux Ratio (R) Against Redshift (z) on Logarithm Scale for the Sample of 242 FR-II Radio Galaxies and 253 Radio-Loud Quasars. (Key: •= Quasars: + = Galaxies).

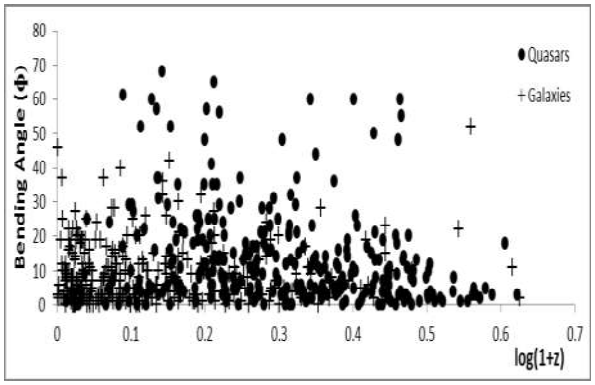

Figure 15: A Scatter Plot of Bending Angle (ϕ) Against Redshift (z) on Logarithm Scale for the Sample of 313 FR-II Radio Galaxies and 308 Radio-Loud Quasars. (Key: •= Quasars: + = Galaxies).

To compare the trend in the cosmological, linear and luminosity evolution of the observed radio source parameter between radio-loud quasars and FR-II radio galaxies, we binned the sample. The original sample is heterogeneous, beside such high luminosity radio sample with luminosity range $(38.86 \leq \log P_{178MHz} \leq 45.89)$ and redshift range $(0.05 \leq z \leq 2.87)$ will allows us to sample different host galaxies with plausible different environment. Thus, we believe that binning will smoothen out randomly induced characteristics/ values in the radio source parameters revealing possible correlations between parameters. One possible problem is the choice of the binning range to obtain nearly equal representation of data. In our analyses, we binned the sample into 8 linear sizes of ranges: $0 \leq D < 50kpc$, $50 \leq D < 100kpc$, $100 \leq D < 150\ kpc$, $150 \leq D < 200kpc$, $200 \leq D < 300\ kpc$, $300 \leq D < 400\ kpc$, $400 \leq D < 700\ kpc$ and $D \geq 700\ kpc$.

We choose the median value of each bin, for our analysis, since it minimizes contributions from outliers. The results of the linear correlation analysis of the binned data are summarized in Table 1. The results seem to indicate that the cosmological evolution of D, P, Q, and ϕ is similar for both classes of radio sources, while the variation of redshift with α and R^* appears different for both classes of radio

Table 1: Correlation Coefficient Results for the Radio Source Parameters Analyzed.

	Galaxies	Quasars		Galaxies	Quasars		Galaxies	Quasars
Parameter	r	r	Parameter	r	r	Parameter	r	r
$z-D$	−0.63	−0.94	$D-\alpha$	0.37	0.33	$P-R^*$	0.83	−0.24
$z-\alpha$	0.30	−0.54	$D-P$	−0.55	−0.97	$P-Q$	0.52	0.85
$z-P$	0.90	0.94	$D-R^*$	−0.47	0.35	$P-\Phi$	0.60	0.87
$z-R^*$	−0.32	−0.10	$D-Q$	−0.34	−0.76	$P-R$	−0.49	0.41
$z-Q$	0.72	0.77	$D-\Phi$	−0.84	−0.85	$P-\alpha$	0.27	−0.44
$z-\Phi$	0.79	0.92	$D-R$	0.21	−0.30			
$z-R$	−0.59	0.49						

sources. Similar trends were observed in size (D) evolution and luminosity (P) evolution with other parameters. Since there is a tight correlation between $P-z$, $P-D$ and $D-z$, the observed trends in the $D-\alpha$, $D-R^*$, $P-\alpha$, and $P-R^*$ correlations might be an artefact of the $P-z$, $P-D$ and $D-z$ correlations.

2.2.2 Luminosity Selection Effect and Linear Size Evolution

The interpretation of the observed angular size-redshift variation ($\theta-z$) of EGRS is often based on linear size cosmological evolution (Oort *et al.* 1987; Kapahi 1989). Earlier studies have shown that the linear size cosmological evolution of the form $D\sim(1+z)^x$ with $x=1-2$, (depending on the value of the density parameter (Ω_0)) is often invoked to interpret the observed data (Barthel & Miley 1988). Analyses by Oort *et al.* (1987), Singal (1993a) and Kapahi (1989) found a strong correlation and a steeper value of $x\sim 3$ for galaxies. Singal (1993b) obtained a result, which indicates that radio galaxies and radio quasars undergo different cosmological size evolution ($x=3.0$ for radio galaxies and $x=0.3$ for radio quasars). Singal (1993b) result clearly contradicts radio source unification scheme in which radio galaxies and radio quasars are expected to differ only in their aspect dependent properties. Several other authors (e.g. Nilsson *et al.* 1993; Nesser *et al.* 1995; Ubachukwu 1998; Ubachukwu & Ogwo 1998; Nilsson 1998; Ubachukwu 2002) had produced results in support of Barthel (1989).

Oort *et al.* (1987) showed that the commonly examined linear size, redshift and emitted radio luminosity power-law relation is of the form:

$$D\propto(1+z)^{-x}P^{y} \quad \ldots 1$$

where x and y are the power index. They were able to separate out the dependence of linear size on redshift from that of radio luminosity. They showed that the median D for radio galaxies, up to $z\sim 1$ varies with P and z, with $x\sim 3$ and $y\sim 0.3$. Kapahi (1989) and Singal (1993a), obtained similar results, but Singal's result also showed that for quasars, $x\sim 0.3$ and $y\sim -0.2$. This result implies that radio galaxies and radio quasars follow different evolutionary trend, which is against the unification scheme. Nilsson *et al.* (1993) found no obvious difference in the $D-P/z$ relations for both quasars and radio galaxies, while Nesser *et al.* (1995) found a milder evolution ($x=1.2\pm0.5$); Ubachukwu & Ogwo (1998) also showed that above a certain critical redshift (z_c), that radio-loud quasars and FR-II galaxies are indistinguishable in their $D-P/z$ relationship and that any linear size cosmological evolution is largely an artefact of the strong luminosity selection effects present in all flux density limited samples.

Ubachukwu *et al.* (1993) have studied the cosmological evolution of luminosities of EGRS and noted that the $P-z$ relation can be approximated to a power-law of the form $P=P_0(1+z)^y$ with y as constant above $z_c\geq 0.3$. Following Ubachukwu & Ogwo (1998), we linearize equation (1) to obtain the variation of linear sizes of EGRSs with radio luminosity and redshift as

$$\log D(P)=a_0\pm y\log P, \quad \ldots 2$$

$$\log D\,(z) = b_0 - x\log(1+z) \quad \ldots 3$$

where a_0 and b_0 are initial value constant. Most analyses usually assume that the exponents x and y are the same everywhere on the $P-z$ plane. Our correlation analyses results showed similar variations between the parameters of FR-II radio galaxies and quasars except for core-dominance and apparent flux ratio. Barthel and Miley (1988) did point out that estimating the $D-z$ relationship over some luminosity range would still leave some residual luminosity effects. To overcome these residual effects, we follow Ubachukwu & Ogwo (1998) to combine equations (2) & (3) to obtain an expression for $D-z$ relationship independent of luminosity effects as

$$\log D\,[P(z)] = a_1 \pm \gamma y \log(1+z) \quad \ldots 4$$

where $a_1 = a_0 \pm y\log P_0$. The interpretation of equation (4) is that if the observed $D-z$ correlation is entirely a luminosity effect, then comparing equations (3) and (4) we have that $x = \gamma y$; otherwise, we obtain $\mu = x \pm \gamma y$; where μ is the residual linear size evolution.

We applied these equations to our sample and our results are: $x = -0.7 \pm 0.5,\ y = -0.04 \pm 0.41,\ \gamma = 4.9 \pm 0.7$ with $\mu = 0.6 \pm 0.2$ and $x = -1.0 \pm 0.5,\ y = -0.03 \pm 0.54,\ \gamma = 8.1 \pm 0.7$ with $\mu = 0.8 \pm 0.2$ for quasars and FR-II radio galaxies respectively. The correlations between $D-P$ and $D-z$ (see Table 1) though strong for both quasars and galaxies are more significant for radio-loud quasars than for FR-II galaxies (with $p = 0.06$ for $D-P$ and $p = 0.02$ for $D-z$ for galaxies, while for quasars $p \leq 1.0 \times 10^{-7}$ for both $D-P$ and $D-z$ correlations). Here p is the probability of getting the given value of r by chance.

The evolutionary trends of both radio-loud quasars and FR-II galaxies are also similar, and within the limits of error, are seemingly the same with $\gamma y = -0.2 \pm 0.4$ for both quasars and FR-II galaxies. The result also indicated a luminosity selection effects up to 40% in quasars, while that in galaxies $\sim 20 - 40\%$. Thus, if the selection effects are properly and equally de-convolved for both classes of object, then observed $D-z$ significant correlation may be an artefact of $P-z$ correlation with no cosmological implication. Onuchukwu (2011a) carried out detailed Spearman partial correlation analysis of P, D and z and obtained a result that suggest that D/z correlation is an artefact of P/z and P/D correlations.

We also followed Ubachukwu and Ogwo (1998) to plot (Figure 16) the median linear size versus luminosity for the entire FR-II galaxies and the radio-loud quasars the binning was done at an interval of $\sim 10^{0.5}\ ergs^{-1}$. The trend shows that both classes of objects are indistinguishable. A polynomial fit to the $P-D$ data gives: $\log D_G = -0.1(\log P)^2 + 6.7\log P - 142.5$ for FR-II radio galaxies and $\log D_Q = -0.1(\log P)^2 + 7.6\log P - 158.4$.

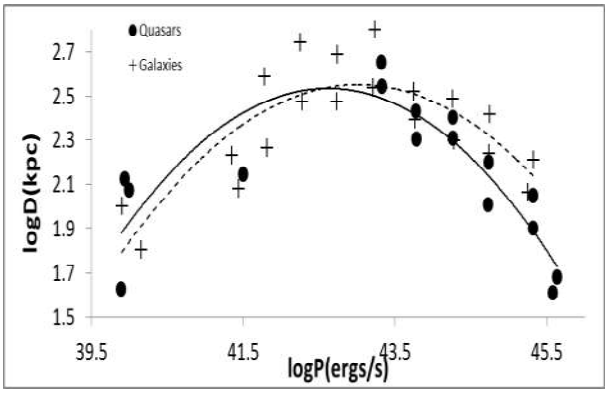

Figure 16: Plot of median value of $\log D$ against $\log P$ with a polynomial fit (Dashed Line: Galaxies; Solid Line: Quasars).

2.2.3. Spectral Index Evolution and Selection Effects

Most of the analyses of spectral index correlation with radio luminosity and redshift had remained inconclusive due to the strong correlation between luminosity and redshift or due to $k-correction$ (e.g. Kapahi & Kulkarni. 1990). The $k-correction$ is a spectrum-dependent correction required because observations are made at a fixed frequency (ν), and we wish to obtain the

power at that frequency, in the frame of the galaxy, bearing in mind that the radiation we observe was emitted at the frequency of $(1 + z)\nu$ (e.g. Leahy 1991).

The variation of spectral index independent of luminosity is best studied using samples of radio sources with approximately the same median luminosity but a wide range of redshifts, this have not been easy to achieve because of the strong correlation between P/z in most flux density limited samples that have been studied. Ubachukwu & Ogwo (1998) gave an expression for studying the variation of spectral indices with redshift (z) and radio luminosity (P) as

$$\alpha(z) = a_2 + m\log(1+z) \quad \ldots 5$$
$$\alpha(P) = b_1 + n\log(P). \quad \ldots 6$$

They pointed out that equations (5) & (6) are true only when the regression parameters m and n are the same at all redshifts and radio luminosities, and if there is no correlation between P/z. The first assumption is approximately correct, but the same cannot be said of the second since in flux density limited samples there is a strong correlation between P/z. To separate the influence of luminosity from the $\alpha - z$ dependence, we follow Ubachukwu & Ogwo (1998) and substitute equation (5) into (6) and obtain an expression for the dependence of α on z independent of P, given by

$$\alpha[P(z)] = a_3 + n\gamma\log(1+z). \quad \ldots 7$$

where a_3 is a constant. It follows from equations (5) and (6) that if the observed $\alpha - z$ relation is entirely due to selection effects, then we can write $m = \gamma n$; otherwise $\sigma = m - \gamma n$; where σ is the residual redshift dependence after correcting for that which results from luminosity selection effects.

We applied equations (5) – (7) to our sample, and our regression analyses results for quasars and galaxies respectively are: $m = 0.3 \pm 0.2$, $n = 0.04 \pm 0.31, \gamma = 4.9 \pm 0.7$ with $\sigma = 0.13 \pm 0.08$ and $m = 0.7 \pm 0.2$, $n = 0.05 \pm 0.21$, $\gamma = 8.1 \pm 0.7$ with $\sigma = 0.24 \pm 0.04$. The result indicates that there is a stronger relation between $\alpha - z$ for galaxies than for quasars, while there seems no strong relation between $\alpha - P$ for both classes of sources.

Our result also indicates that $\sim 73\%$ of spectral steeping in FR-II contained in our sample is due to selection effects, while that of radio-loud quasars is $\sim 87\%$. Though the errors in our results are significant, it also suggests that selection effects are largely responsible for any spectral index evolution with epoch for both classes of object.

We also plotted the median spectral index against extended luminosity (Figure 17) for both classes of objects. The binning was done in an interval of $\alpha = 0.1$. The plot shows a large steepening of spectral index for both radio-loud quasars and FR-II galaxies, regression fit to the median $\alpha - P$ data gives: $\alpha = \alpha_0 \log P^{0.4\pm0.2}$ and $\alpha = \alpha_0 \log P^{0.3\pm0.2}$ for quasars and FR-II galaxies respectively. The trend in the data is similar except that quasars have higher luminosities. We performed similar plot for the median $\alpha - z$ data with plot shown in Figure 18, the regression fit respectively for quasars and FR-II galaxies gives : $\alpha = \alpha_0(1+z)^{1.3\pm0.2}$ and $\alpha = \alpha_0(1+z)^{1.3\pm0.1}$. Again, the trend is similar for both classes of objects, except that quasars occur at higher redshifts. This result may offer no new physics to understanding EGRS, but it indicates that evolution in luminosity (P) manifested by evolution in spectral index (α) is the same for both FR-II galaxies and radio-loud quasars, which is in favor of unification scheme.

2.2.4 Aspect-Dependent Properties of Radio-Loud Quasars and FR-II Radio Galaxies

Clearly unification of FR-II radio galaxies and radio-loud quasars would predict that, on the average, the extended radio emission from quasars should appear concentrated in smaller regions than that coming from FR-II radio galaxies because of projection effects. However, Singal (1993b), finds that for low luminosity ranges, the mean sizes of radio-loud quasars are larger than those of FR-II galaxies. This

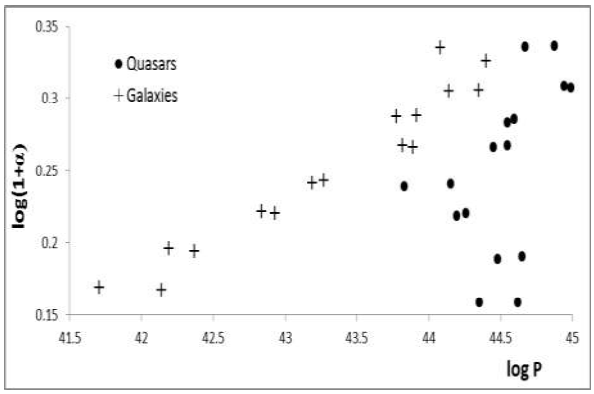

Figure 17: Plot of median value of $\log(1+\alpha)$ against $\log P$.

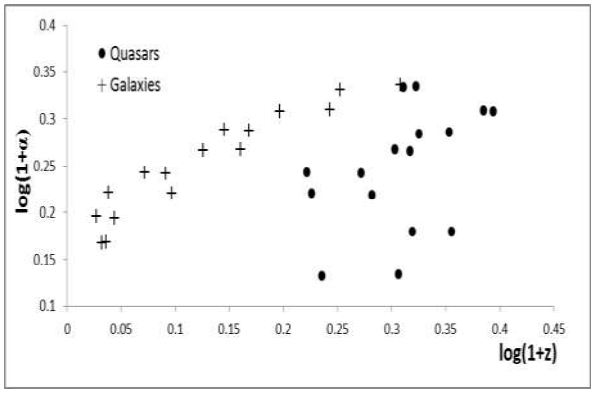

Figure 18: Plot of median value of $\log(1+\alpha)$ against $\log(1+z)$.

result is the direct opposite of that predicted by unification. Moreover, his result also finds appreciable differences in the $P-z$ and $D-z$ correlations. These results however, are not conclusive due to the incompleteness of the sample and uncertainties in the actual definition of linear size for such low luminosity sample (Nilsson *et al*. 1993). Ubachukwu (2002) showed that for any evolving Friedmann universe, the linear size of a radio source is related to its largest angular size (θ) through

$$D = \Psi(\Omega,z)\theta, \qquad \ldots 10$$

where $\Psi(\Omega,z)$ is a known function of redshift (z) for any given cosmological model parameterized by the density parameter (Ω) and the largest observed angle size (θ) of the radio source. If the radio axis of the source makes an opening angle (φ) with respect to the line of sight, following Ubachukwu (2002), we can write

$$D = D_0 \sin\varphi, \qquad \ldots 11$$

where D_0 is the intrinsic linear size of the source. We assume that D_0 should be approximately the same for radio-loud quasars and FR-II galaxies when matched in the $P-z$ plane if the unification scheme is correct. With that assumption, we can write the equation for the foreshortening factor F as

$$F = \frac{\sin\varphi_g}{\sin\varphi_q} = \frac{D_0 \sin\varphi_g}{D_0 \sin\varphi_q} = \frac{D_g}{D_q} \qquad \ldots 12$$

where φ_g and φ_q are the median opening angles, D_g and D_q are the median sizes of FR-II galaxies and radio-loud quasars respectively. Using equation (12), we calculated the median value of the linear sizes for both classes of object and evaluate the foreshortening factor F. Our results for all redshift range $(0.00 \leq z \leq 2.88)$ is $F = 1.87$, which is in good agreement with the result obtained by Ubachukwu (2002) using the core dominance parameter (R^*) to obtained a value of $F = 1.7$ and Barthel (1989) using the relative number and liner sizes to obtain $F \sim 1.8$.

3.0 Discussion and Conclusion

From the distribution plot, the linear size distribution of both classes of object appears similar. After the initial increase in the number density with increase in liner size, the number of radio sources decreases with increasing linear size. The luminosity distribution indicates that radio-loud quasars are more luminous than FR-II galaxies, also more quasars are found at higher redshifts than FR-II galaxies. The spectral index distribution is completely matched for both classes of object. Generally, radio-loud quasars show more asymmetries than FR-II galaxies. This can be understood in the context of beaming theory (e.g. Barthel 1989). Another factor responsible for this apparent difference could be attributed to selection effects, since in our sample, quasars are located in denser environment than galaxies with the density of universe varying as $(1+z)^{\rho}$, with ρ positive; Onuchukwu (2011b).

The coefficient of correlation using the median values of the parameters analyzed showed similar trends between $z-D, z-P, z-Q, z-\phi, D-P, D-\alpha, D-\phi, P-Q,$

and $P-\phi$, for both classes of objects, but the trends differ between $z-\alpha, z-R^{c}, z-R, D-R, D-R^{c}, P-R^{c}, P-R$ and $P-\alpha$. The trends differ only when parameters involving interactions with environments as represented by the spectral index are analyzed, indicating that either the host galaxies of radio-loud quasars and FR-II radio galaxies may be different. Alternatively, our sample which is bias towards higher redshift for radio-loud quasars than FR-II radio galaxies could be the source of the observed difference in the asymmetry parameters analyzed. Studies have shown that environmental factors are important in explaining observed asymmetries in radio sources (e.g. Laing 1988; Antonucci 1993; Teerikorpi 2001, Onuchukwu & Ubachukwu 2013). Since radio-loud quasars are situated at larger redshifts than FR-II radio galaxies ($z_m = 0.411$ for FR-II and $z_m = 1.043$ for quasars), this may be responsible for the observed differences in the variation of the asymmetry parameters with other radio source parameters for the two classes of radio sources.

Further analyses of $P-D$, $\alpha-P$, and $\alpha-z$ indicate that for both radio-loud quasars and FR-II radio galaxies, the $P-D$, $\alpha-P$, and $\alpha-z$ relations are significantly the same (see Figures 15-17). At low luminosities the $D-P$ plot shows that for both quasars and FR-II galaxies, there is an indication of an initial increase in D up to about $\log D = 2.6\ (kpc)$, then thereafter declines as luminosity increases. Similar plots of medium α versus P and α versus z show similar trend in variation for both classes of object. These analyses indicate that when properly matched in parameter planes, the evolution in linear size, (D), luminosity (P) and spectral index (α) are similar for both radio-loud quasars and FR-II radio galaxies. This result is in agreement with Nesser *et al*. (1995), Ubachukwu and Ogwo (1998) and Ubachukwu (2002).

Statistically, for any random oriented radio sources, the number statistics and the aspect angle of beamed counter-part are expected to be smaller than those of the parent objects (Barthel 1989). Barthel (1989), showed that the median aspect angle for the beamed radio-loud quasars is $\varphi_q \sim 31^{\circ}$, and that of FR-II galaxies is $\varphi_g \sim 69^{\circ}$, giving a foreshortening factor of $F \sim 1.8$. Ubachukwu (2002) obtained a similar result with $\varphi_q \sim 28^{\circ}$ and $\sim 51^{\circ}$ for radio-loud quasars and FR-II galaxies respectively giving a foreshortening factor of ~ 1.7. We assumed that the linear sizes of radio sources are independent of redshift, and followed Ubachukwu (2002) to related the linear size of a radio source with its aspect angle, obtained a foreshortening factor $F \sim 1.87\ (0 < z \leq 2.88)$.

In conclusion, our analyses of extended linear size (D), extended luminosity (P), spectral index (α), redshift (z) and the asymmetry parameters show that radio-loud quasars can be regarded as the beamed/less oriented counter-part of FR-II galaxies, similar to the conclusion of Barthel (1989). One of the major arguments against unification is the observation that there are intrinsic differences in the behavior of radio-loud quasars and FR-II galaxies at low redshifts in the $D-P/z$ relationships (Singal 1993a). However Gopal-Krishna (1996) attributed these apparent differences to the temporal evolution in both luminosities and linear sizes of radio sources. Ubachukwu and Ogwo (1998) also pointed out that the observed inconsistencies in the $D-P/z$ relations may disappear if the two classes of objects are matched in their $P-z$ plane a result that is consistent with our analyses.

References

Antonucci, R. 1993, "Unified Models for Active Galactic Nuclei and Quasars" ARAA, **31**, 473-521

Barthel, P.D. 1989, "Quasars and Radio Galaxies May be Two of a Kind" ApJ, **336**, 606-616.

Barthel, P.D., and Miley, G.K. 1988, "Evolution of Radio Structure In Quasars – A New Probe of Protogalaxies" Nature, **333**, 319-330

Blandford, R. D., & Znajek, R. L. 1977, "Electromagnetic extraction of energy from Kerr black holes", MNRAS, **179**, 433-456

Blandford, R. D., & Payne, D. G. 1982, "Hydromagnetic flows from accretion discs and the production of radio jets", MNRAS, **199**, 883-903.

Blundell, K.M., Rawlings, S., & Willott, C.J. 1999, "The Nature and Evolution of Classical Double Radio Sources from Complete Samples", AJ, **117**, 677-706

Britzen, S., Vermeulen, R.C., Campell, R.M., Taylor, G.B., Pearson, T.J., Readhead, A.C.S., Xu, W., Browne, I.W.A., Henstock, D.R., & Wilkinson, P. 2008, "A multi-epoch VLBI survey of the kinematics of CFJ sources II. Analysis of the kinematics", A&A **484**, 119–142

Fanaroff, B.L., and Riley, J.M. 1974, "The Morphology of Extragalactic Radio Sources of High and Low luminosity", MNRAS, **169**, 310-319.

Gopal-Krishna. 1996, "Unified Schemes For Extragalactic Radio Sources, in "Extragalactic radio Sources" IAU Symp. **175**. (Eds. R. Ekers *et al*.) Kluwer Academic, Dorchrecht. pp563

Kapahi, V.K. 1989, "Redshift and Luminosity Dependence of Linear Sizes of Powerful Radio Galaxies", AJ, **97**, 1-8

Kapahi, V.K., and Kullkarni, V.K. 1990, "VLA Observations of Unidentified Leden-Berkeley Deep-Survey Sources – Luminosity and Redshift Dependence of Spectral properties", AJ, **99**, 1397-1403.

Lobanov, A.P., & Zensus J.A., 2006, Active Galactic Nuclei at the cross road of Astrophysics **arXiv:astro-ph/06061431**, 1-16

Laing, R.A. 1988, "The Sidedness of Jets and Depolarization in Powerful Extragalactic Radio Sources", Nature, **331**, 149-160

Leahy, J.P., 1991, 'Interpretation of Large Scale Extragalactic Jets in "Beams and Jets in Astrophysics". Ed. P.A. Hughes, Cambridge University Press, Cambridge.

Lehnert, M.D., Heckman, T.M., Chamber, K.C., and Miley, G.K. 1992, "Multicolor Images of Spatially Resolved Structures Around High-Redshift Quasars", ApJ, **393**, 68-88.

Liu, Y., Jiang, D.R., and Gu, F.G., 2006, "The Jet Power, Radio Loudness, and Black Hole Mass in Radio-Loud Active Galactic Nuclei", ApJ, **637**, 669–681,

McCarthy, P.J., Spinard, A., and Van Breguel, W.J. 1995, "Emission-Line Imaging of 3CR Radio Galaxies", ApJS, **99**, 27-35.

Magorrian, J., Tremaine, S., Richstone, D., Bender, R., Bower, G., Alan Dressler, A., Faber, S. M., Gebhardt, K., Green, R., Grillmair, C., Kormendy, J. and Lauer, T. 1998, "The Demography Of Massive Dark Objects In Galaxy Centers", AJ, **115**, 2285-2305

Nesser M.J., Eales, S.A., Law-Green, J.D., Leahy, J.P., and Rawlings, S. 1995, "The Linear Size Evolution of Classical Double Radio Sources", ApJ, **451**, 76-86.

Nilsson, K. 1998, "Kinematical Models of Double Radio Sources And The Unified Scheme. A&ASS", **132**, 31-.37

Nilsson, K., Valtones, M.J., Kotilaimen, J., Kaakkola, T. 1993, "On the Redshift-Apparent Size Diagram of Double Radio Sources", ApJ, **413**, 453-470.

Onuchukwu, C. C., 2011a, "Statistical Correlation of EGRS Parameters", Journal of Basic Physical Research **Vol. 2, No. 2**, 14-20

Onuchukwu, C. C., 2011b, "Asymmetries in Extragalactic Radio Sources", Journal of Basic Physical Research **Vol. 2, No. 1**, 43-49

Onuchukwu, C. C., & Ubachukwu, A.A. 2013, "Structural Asymmetries, Relativistic Beaming and Orientation Effects in Lobe-Dominated Quasars", Ap&SS **344**, No 1, 211-218, DOI 10.1007/s10509-012-1325-x,

Oort, M.J.A., Kartgert, P., and Winhorst, R.A. 1987, "A Direct Determination of Linear Size Evolution of Elliptical Radio Galaxies", Nature, **328**, 500-510.

Singal, A.K. 1993a, "Evidence against the Unified Scheme for Powerful Radio Galaxies and Quasars", MNRAS, **262**, 27-31

Singal, A.K. 1993b, "Cosmic Evolution and Luminosity Dependence of the Physical Sizes of Powerful Radio Quasars" MNRAS, **263**, 139-150.

Smith, E.P., and Heckman, T.M. 1989, "Local Environment of Low Redshift QSOs and Powerful Radio Galaxies", BAAS, **21Q**, 777-784.

Teerikorpi, P. 2001, "Evidence for the Class of the most Luminous Quasars III. Linear Size and core-size relation of double radio sources", A&A **375**, 752-760

Ubachukwu, A.A. 1998, "Spectral Index Asymmetries in Powerful Radio Sources: Cosmological Evolution versus Luminosity Selection Effects", IAJ, **25**, 25-28.

Ubachukwu, A.A. 2002, "Statistical Tests of the Unification Scheme for High-luminosity Double Radio Sources" AP&SS, **279**, 251-259.

Ubachukwu, A.A., and Ogwo, J.N. 1998, "Luminosity Selection Effects and Linear Size Evolution in the Quasar/Galaxy Unification Scheme" AJP, **51**, 143-151.

Ubachukwu, A.A., Okoye, S.E., Onuorah, L.I. 1993, "Radio Source Orientation and the Cosmological Interpretation of the Angular Size – Redshift Relation For Double-lobed Quasars" Ap&SS, **209**, 169-175.

Urry, C.M., and Padovani, P. 1995 "Unified Schemes for Radio-loud AGNs". ASP, **107**, 803-845

Willot, C.J., Rawlings, S., Blundell, K.M., and Lacy, M. 1998, "The Luminosity Function Of Radio-loud Quasars from the 7C Redshift Survey", MNRAS, **300,** 625-648.